Influence de la température de rotation sur les branches P, Q et R du spectre d'émission du système $^2\Sigma \rightarrow {}^2\pi$ du radical hydroxyde OH

Samuel Ouoba, Justin Zaïda, Ouindpouiré Auguste Aristide Soré, Jean Koulidiati

Journal de la Société Ouest-Africaine de Chimie
J. Soc. Ouest-Afr. Chim. (2022), 051 : 66 - 77
27ème Année, 2022

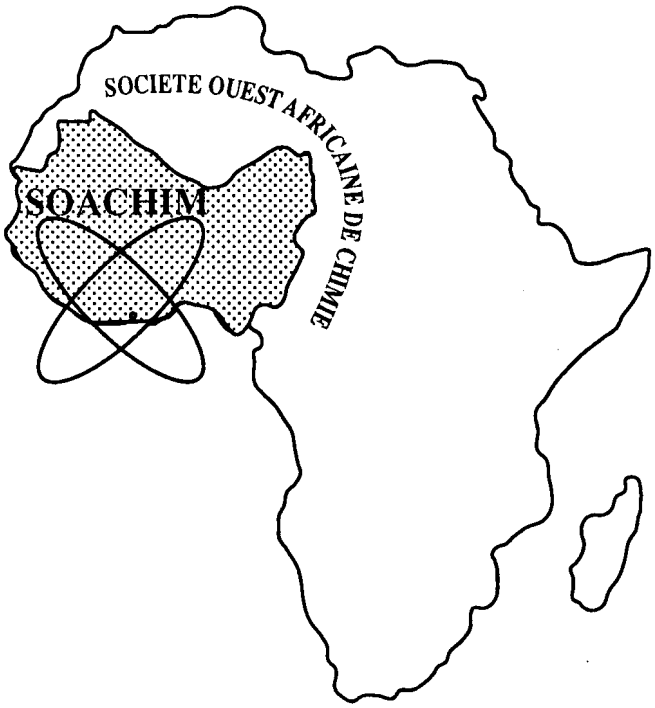

ISSN 0796-6687
Code Chemical Abstracts : JSOCF2
Cote INIST (CNRS France) : <27680>
Site Web: **http://www.soachim.org**

Influence de la température de rotation sur les branches P, Q et R du spectre d'émission du système $^2\Sigma \rightarrow {}^2\pi$ du radical hydroxyde OH

Samuel Ouoba*, Justin Zaïda, Ouindpouiré Auguste Aristide Soré and Jean Koulidiati

Laboratoire de Physique et de Chimie de l'Environnement, Université Joseph KI-ZERBO, UFR-SEA, 03 BP 7021 Ouaga 03, Burkina Faso

(Reçu le 20/05/2022 – Accepté après corrections le 25/11/2022)

Résumé : Le travail de cet article porte sur l'influence de la température de rotation sur les spectres d'émission des branches relativement à la tête de bande Q(0,0). Après avoir décrit les états de rotation, nous avons pris en compte le moment cinétique total dans le cas où le spin électronique est négligé. Nous avons ensuite déterminé les termes d'énergie et le nombre d'onde en définissant les différents niveaux d'énergie. Nous avons également défini la règle de sélection des différentes transitions en prenant en compte les transitions qui satisfont à cette règle. Trois branches fortes et dix branches ou nombres d'onde ont été définis. Nous avons ensuite défini la distribution des intensités de raies ou probabilité de transition en fonction du nombre quantique de rotation. Enfin, nous avons déterminé l'intensité d'une raie de rotation basée sur les transitions entre les niveaux de rotation appartenant à deux niveaux d'énergie vibrationnelle. Les résultats numériques montrent que le spectre d'émission est insensible aux températures de rotation inférieures à 62,67 K pour toutes les branches et aux températures de rotation supérieures à 850 000 K, 750 000 K et 650 000 K respectivement pour les branches Q, P et R.

Mots clés : longueur d'onde ; niveaux d'énergie; modèle numérique ; radical OH ; spectre ; Température rotationnelle

Influence of rotational temperature on emission spectra of the branches Q, P and R of the system $^2\Sigma \rightarrow {}^2\pi$ of hydroxide radical OH

Abstract: The work of this paper is focused on the influence of rotational temperature on the emission spectra of the branches relatively to the head of band Q(0,0). After a description of the rotational states, we took into account the total angular momentum in the case where the electronic spin is neglected. We then determined the terms of energy and the wave number by defining the different levels of energy. We have also defined the selection rule for the different transitions by only taking into account the transitions which satisfy this rule and then three main branches are defined. Considering these strong branches, ten branches or wavenumbers have been defined. We have defined the distribution of line strengths or transition probability as a function of the rotational quantum number. Finally, we have determined the intensity of a rotational line based on the transitions between rotational levels belonging to two vibrational energy levels. The results show that the emission spectra is insensitive to rotational temperatures lower than 62.67 K for all the branches and to rotational temperatures higher than 850,000 K, 750,000 K, and 650,000 K respectively for the branches Q, P and R.

Keywords: Energy Levels; Spectra; Rotational Temperature; OH-radical; Numerical Model.

* Coresponding Author : S. OUOBA, samuel_ouoba1@yahoo.fr

List of Symbols

a	coupling constant
B	characteristic constant of the state
b_1	characteristic constant of the state
c	speed of light
D	characteristic constant of the state
E	total energy
E_e	electronic energy
E_r	rotational energy
E_v	vibrational energy
F_1	rotational levels of the $^2\Sigma$ state
F_2	rotational levels of the $^2\Sigma$ state
f_1	rotational levels of the $^2\pi$ state
f_2	rotational levels of the $^2\pi$ state
F'	rotational energy of the level $^2\Sigma$
f_1'	energy levels due to the splitting
f_2'	energy levels due to the splitting
h	Planck's constant
I	relative intensity
J	total angular momentum
K	angular momentum
k	Boltzmann's constant
m	Mass of molecules
N	molecules number
P_1	Main branch
P_{12}	satellite branch
P_2	Main branch
Q_1	Main branch
Q_{12}	satellite branch
Q_2	Main branch
Q_{21}	satellite branch
R	characteristic constant of the state
R_1	Main branch
R_2	Main branch
R_{21}	satellite branch
T	Temperature
T_r	rotational temperature
U	spectral density
v	Molecules velocity

Greek Symbols

ε	spectral emission power
λ	Wavelength
ν	Frequency
σ	wave number

1. Introduction

Under certain conditions of excitation, a system can emit a molecular spectra characterized by a series of grooves or luminous bands presenting on one side a clear limit and degraded on the other side [1-3].

A plasma is a state of matter where the atoms are totally or partially ionized. It is a mixture of molecules, atoms, ions and electrons whose state can be defined as a function of temperature [4-8]. There are plasmas in equilibrium and plasmas out of equilibrium.

A plasma in complete thermodynamic equilibrium is a plasma whose macroscopic parameters do not vary as long as the external conditions remain unchanged. Consequently all the particles are in equilibrium with each other and with the walls of the enclosure at a temperature T.

The spectroscopic analysis of the radiation emitted by a plasma is an excellent means of diagnosis [9, 10] because it does not disturb the plasma [11, 12]. Its only flaw is the impossibility of detecting non-radiative states. To determine the temperature of a plasma, several spectroscopic methods are proposed in the literature [13, 14].

Our work will consist in studying the influence of the rotational temperature on the molecular spectra of hydroxide radical OH using a numerical simulation model. The simulation method was validated by one of our previous publications [2]. Indeed, the simulation of molecular bands is not novelty because it has already been used by Smit-Miessen et al. [15]. However, with the development of computers, it is possible to make this technique more efficient, particularly in the comparison of theoretical spectra with experimental spectra which makes it possible to determine one or more parameters of a plasma.

Regarding molecular spectra, the total energy is defined as the sum of three terms [3].

$$E = E_e + E_v + E_r \quad (1)$$

There is emission or absorption of a photon of frequency ν given by Einstein's relation ($\Delta E = E - E' = h\nu$) when the system passes from state E to state E'.

Thus a very weak excitation i.e. of the order of 10^{-3} eV corresponding to photons with wavelength close to 1 mm, therefore located in the micro waves domain or far infrared causes transitions between rotational levels only [16, 17]. We thus obtain spectra of pure rotation.

A slightly more energetic excitation (about 0.3 eV or $\lambda \approx 3.6$) makes it possible to modify not only the quantum state of rotation but also the quantum state of vibration. We thus obtain spectra of vibration – rotation.

A more intense excitation i.e. about few eV makes it possible to obtain electronic transitions.
With regard to the latter, it should be noted that for the molecule as for the atom, the probability of simultaneous excitation of two electrons is extremely low.
The work we present in this article deals with the influence of rotational temperature on emission spectra of the branches Q, P and R of the system $^2\Sigma \rightarrow {}^2\pi$ of hydroxide radical OH. After doing a theoretical study of the OH radical, we presented the simulation procedure of molecular spectra. Several results obtained for a wide range of temperature have been presented and extensively commented on.

2. Theory about the hydroxide radical OH

2.1 Structures of the bands $^2\Sigma \rightarrow {}^2\pi$ of the hydroxide radical OH

The description of the rotational states of any diatomic molecule requires the consideration of the total angular momentum J or the angular momentum K when the electronic spin is neglected. Vector K whose norm is always an integer makes it possible to describe the movement of the nuclei when the interaction between the electronic spin and the rest of the molecule is weak. But it could also be used in any case assuming that it represents the angular momentum without interaction between spin and molecular orbital. If the resultant of the orbital angular momentum $\Lambda \neq 0$, two cases called Hund's cases must be considered [18].

- Case (a): the spin is coupled through the orbital angular momentum to the inter-nuclear axis. The rotational energy is defined to within an additive constant BJ (J+1),
- Case (b): the rotation is very strong such that the spin is coupled to the axis of rotation rather than to the inter-nuclear axis. In this approximation, the rotational energy is B[K(K+1)-Λ^2].

For K to be considered as a number describing the rotational states of a molecule, it is necessary to use case (b) of Hund's nomenclature. This is interesting because it characterizes the state Σ for which $\Lambda=0$. On the other hand, the state π being characterized by $\Lambda \neq 0$, it is more judicious to use case (a) and case (b) of Hund's nomenclature.

2.2 Energy terms and wave number of the system $^2\Sigma \rightarrow {}^2\pi$ of the hydroxide radical OH

The energy levels used in this work are defined as followed:

- **For the state $^2\Sigma$**

$$F_1(K) = BK(K+1) - DK^2(K+1)^2 + R\left(K+\frac{1}{2}\right) \quad (2)$$

$$F_2(K) = BK(K+1) - DK^2(K+1)^2 - R\left(K+\frac{1}{2}\right) \quad (3)$$

Where B, D and R are the characteristic constants of the state.

- **For the state $^2\pi$**

$$f_1(K) = B\left[(K+1)^2 - 1 - \frac{1}{2}\sqrt{4(K+1)^2 + a(a-4)}\right] - DK^2(K+1)^2 \quad (4)$$

$$f_2(K) = B\left[K^2 - 1 + \frac{1}{2}\sqrt{4K^2 + a(a-4)}\right] - DK^2(K+1)^2 \quad (5)$$

Where a is called coupling constant.
Taking into account this coupling we can write:

$$f_1'(K) - f_1(K) = b_1K(K+1) \quad (6)$$
$$f_2'(K) - f_2(K) = b_1K(K+1) \quad (7)$$

Where $f_1'(K)$ and $f_2'(K)$ are energy levels due to the splitting Λ.

The selection rule for the transition $^2\Sigma \rightarrow {}^2\pi$ is K+1→K, K→K and K-1→K i.e. $\Delta K=0$ or $\Delta K=\pm 1$. The transitions which satisfy this rule are called strong branches and those which do not satisfy this selection rule are called weak branches. This allows us to obtain three strong main branches given by:
P Branch for $K-1 \rightarrow K$
Q Branch for $K \rightarrow K$
R Branch for $K+1 \rightarrow K$
There are also satellite branches which are characterized by two indices and denoted by P_{ij}, Q_{ij}, R_{ij} with i,j=1,2 such that i≠j. Considering only the strong branches, the following ten branches called wavenumbers have been defined [19, 20]:

$$P_1(K) = F_1(K-1) - f_1(K) \quad (8)$$
$$P_2(K) = F_2(K-1) - f_2(K) \quad (9)$$
$$P_{12}(K) = F_1(K-1) - f_2(K) \quad (10)$$
$$Q_1(K) = F_1(K) - f_1'(K) \quad (11)$$
$$Q_{21}(K) = F_2(K) - f_1'(K) \quad (12)$$
$$Q_2(K) = F_2(K) - f_2'(K) \quad (13)$$
$$Q_{12}(K) = F_1(K) - f_2'(K) \quad (14)$$
$$R_1(K) = F_1(K+1) - f_1(K) \quad (15)$$
$$R_{21}(K) = F_2(K+1) - f_1(K) \quad (16)$$
$$R_2(K) = F_2(K+1) - f_2(K) \quad (17)$$

2.3 Molecular constants

The constants R, B and D of $^2\Sigma$ state and B, D, a and b_1 of $^2\pi$ state are given in table 1.

Table 1: Molecular constants for the system $^2\Sigma \rightarrow {}^2\pi$.

Constants	*B*	*D*	*R*	*a*	b_1
State $^2\Sigma$	16.961	0.00204	0.1122	-	-
State $^2\pi$	18.515	0.00187	-	-7.547	0.0417

2.4 Line force distribution

The strengths of the lines or transition probability essentially depend on the rotation quantum number J and the coupling constant a. They have been determined by Earls [18] and Leaner [21] by considering the expressions of the energy levels given by Hill and Van Vleck [22].

$$R_2 = \frac{2J+1}{2J+2}\{(2J+1) + U[(2J+1)^2 - 2a]\} \quad (18)$$

$$\begin{Bmatrix} R_1 \\ Q_{12} \end{Bmatrix} = \frac{2J+1}{2J+2}\{(2J+1) \pm U[(2J+1)^2 + 2(a-4)]\} \quad (19)$$

$$\begin{Bmatrix} Q_2 \\ R_{21} \end{Bmatrix} = \frac{2J+1}{2J+2}\left\{\frac{(2J+1)^2 - a \pm U[(2J+1)^3 - 8J - 2a]}{J}\right\} \quad (20)$$

$$\begin{Bmatrix} Q_1 \\ P_{12} \end{Bmatrix} = \frac{2J+1}{2J+2}\left\{\frac{(2J+1)^2 - 2 \pm U[(2J+1)^3 - 8J + 2(a-4)]}{J}\right\} \quad (21)$$

$$P_1 = \frac{2J+1}{2J}\{(2J+1) + U[(2J+1)^2 - 2a]\} \quad (22)$$

$$\begin{Bmatrix} P_2 \\ Q_{12} \end{Bmatrix} = \frac{2J+1}{2J}\{(2J+1) \pm U[(2J+1)^2 + 2(a-4)]\} \quad (23)$$

Where

$$U^{-1} = \sqrt{(2J+1)^2 + a(a-4)} \quad (24)$$

In these formulas, the sign + which precedes U is put for the main branches and the sign – is used for the satellite branches. The formulas are arranged in pairs and the values of J correspond to the final state 2π.

2.5 Intensity of a rotational line

By focusing on the transitions between rotation levels belonging to two fixed vibrational energy levels, we obtain the relative intensity I(J) of a rotational line in the following form :

$$I(J) = \sigma^4 S_{J'J''} \exp\left(-\frac{hcF'(J)}{kT_r}\right) \quad (25)$$

Where F'(J) represents the rotational energy of level $^2\Sigma$, Tr the rotational temperature, σ the wave number of an individual line and S the strength of the line.

3. Molecular spectra simulation procedure

The simulation of emission spectra is very useful because it allows to identify the molecules. It also makes it possible to determine the rotational temperatures of a molecule by comparing intensities and positions of the rotational lines of the simulated and experimental spectra.

For the simulation of the emission spectra of hydroxide radical OH, we followed the seven (07) steps proposed by Ouoba et al. [2] :

- First, we calculate the spectral terms of rotation of each state and each doublet, taking into account the splitting of the spin, the splitting of lambda, the term taking into account the large rotations,
- We then calculate the wavelengths of branches P, Q and R responding to the selection rules listed in the previous paragraphs,
- We establish the expressions of the forces of lines using the classical formulas of Earls [18],
- We determine the different molecular constants of the different states,
- We define a scale such that all the lines which have their wavelengths included in the same interval have their intensities integrated. The representation, as a function of wavelengths, of the integrated intensity of the different lines gives us an ideal spectra. We finally obtain a Dirac comb each having its own intensity,
- We take into account the device profile which plays an essential role experimentally. In the majority of cases, a slit of the spectral device gives a Gaussian spectral profile of half width DX at 1/e height. This half-width becomes an essential parameter of the simulation program,
- We finally proceed to the numerical convolution of each Dirac peak with the Gaussian profile and we obtain the final simulated spectrum having the parameters DX and Tr.

4. Results and discussion

In order to compare the results of simulation with those of the experiment, the spectroscopic study was conducted in the infrared characterized by wavelengths ranging between 3064.6 Å and 3331 Å. We present the results of wavelengths (Table 2) and Holn London factors (Table 3), respectively. The results of these two tables are in very good agreement with the results published by Dieke and Crosswhite [19].

4.1. Influence of rotational temperature on the spectra of the P, Q and R branches

To study the influence of rotational temperature on the branches P, Q and R, we varied the values of rotational temperature in a wide range between Tr=0 K and Tr=10,000.000 K. In a first time we represented the variation curves of the normalized average value of intensity of the branches Q, P and R as a function of the rotational temperature for Tr values ranging between 0 K and 100 K. We have noticed that the emission spectra is not sensitive for Tr varying from 0 K to 62.5 K but sensitive for Tr=63 K. In order to determine the minimum limiting value from which the spectra is sensitive to the rotational temperature, we restricted the interval of study of the normalized average value of intensity between 62.5 K to 63 K (**Figures 1, 2 and 3**). The results of those figures show that for the three branches Q, P and R the lowest sensitive rotational temperature is $T_r^{min} = 62.67$ K. We present the normalized simulated spectra of branches P, Q, and R for a rotation temperature $T_r = T_r^{min}$ (**Figure 4**).

Table 2: Wavelengths (Å) obtained by simulation.

K	λ_{P1}	λ_{P2}	λ_{P12}	λ_{Q1}	λ_{Q21}	λ_{Q2}	λ_{Q12}	λ_{R1}	λ_{R21}	λ_{R2}
1	3082.6	3094.7	3094.7	3079.3	3079.4	3091.4	3091.4	3072.9	3072.9	3085.0
2	3087.3	3097.3	3097.2	3080.9	3080.9	3090.8	3090.8	3071.2	3071.3	3081.1
3	3092.1	3100.5	3100.4	3082.5	3082.5	3090.8	3090.7	3069.6	3069.7	3077.9
4	3097.0	3104.2	3104.1	3084.2	3084.3	3091.3	3091.2	3068.2	3068.3	3075.2
5	3102.2	3108.4	3108.3	3086.1	3086.3	3092.3	3092.2	3066.9	3067.1	3073.1
6	3107.5	3113.0	3112.9	3088.3	3088.4	3093.8	3093.6	3065.9	3066.1	3071.3
7	3113.1	3118.0	3117.9	3090.7	3090.9	3095.6	3095.5	3065.2	3065.4	3070.0
8	3118.9	3123.4	3123.2	3093.4	3093.6	3097.8	3097.7	3064.7	3064.9	3069.1
9	3125.0	3129.1	3128.9	3096.4	3096.6	3100.4	3100.2	3064.6	3064.8	3068.6
10	3131.3	3135.2	3134.9	3099.6	3099.9	3103.4	3103.2	3064.8	3065.0	3068.5
11	3138.0	3141.5	3141.3	3103.2	3103.5	3106.7	3106.5	3065.3	3065.6	3068.8
12	3144.9	3148.3	3148.0	3107.1	3107.4	3110.4	3110.2	3066.2	3066.5	3069.4
13	3152.1	3155.3	3155.0	3111.4	3111.7	3114.5	3114.2	3067.5	3067.8	3070.5
14	3159.7	3162.7	3162.4	3116.0	3116.3	3118.9	3118.6	3069.1	3069.4	3072.0
15	3167.5	3170.4	3170.1	3120.9	3121.2	3123.7	3123.4	3071.1	3071.5	3073.9
16	3175.7	3178.4	3178.1	3126.2	3126.6	3128.9	3128.6	3073.6	3073.9	3076.2
17	3184.2	3186.8	3186.5	3131.9	3132.3	3134.5	3134.1	3076.4	3076.8	3079.0
18	3193.0	3195.6	3195.2	3138.0	3138.4	3140.5	3140.1	3079.7	3080.1	3082.2
19	3202.1	3204.7	3204.2	3144.5	3144.9	3146.9	3146.5	3083.5	3083.9	3085.9
20	3211.7	3214.1	3213.7	3151.4	3151.8	3153.8	3153.3	3087.7	3088.2	3090.0
21	3221.5	3224.0	3223.5	3158.7	3159.2	3161.0	3160.5	3092.4	3092.9	3094.7
22	3231.8	3234.2	3233.7	3166.5	3167.0	3168.8	3168.3	3097.6	3098.1	3099.8
23	3242.4	3244.8	3244.2	3174.7	3175.2	3177.0	3176.4	3103.3	3103.9	3105.5
24	3253.5	3255.8	3255.2	3183.4	3184.0	3185.6	3185.1	3109.6	3110.2	3111.7
25	3264.9	3267.2	3266.6	3192.6	3193.2	3194.8	3194.2	3116.4	3117.0	3118.5
26	3276.8	3279.0	3278.4	3202.3	3203.0	3204.5	3203.9	3123.9	3124.5	3125.9
27	3289.1	3291.3	3290.7	3212.6	3213.2	3214.7	3214.1	3131.9	3132.5	3133.9
28	3301.9	3304.1	3303.4	3223.4	3224.1	3225.5	3224.9	3140.5	3141.2	3142.6
29	3315.1	3317.3	3316.6	3234.8	3235.5	3236.9	3236.2	3149.9	3150.5	3151.9
30	3328.8	3331.0	3330.3	3246.8	3247.5	3248.9	3248.2	3159.9	3160.6	3161.9

Table 3: Holn London factors obtained by simulation.

K	σ_{P1}	σ_{P2}	σ_{P12}	σ_{Q1}	σ_{Q21}	σ_{Q2}	σ_{Q12}	σ_{R1}	σ_{R21}	σ_{R2}
1	9.4155	-0.0000	5.3333	8.9846	6.2647	16.9454	2.6667	2.6412	9.0350	2.6667
2	12.7251	4.4020	5.9487	16.9993	5.8044	15.6617	3.7588	6.1397	8.4084	5.6493
3	16.4954	8.5956	6.3150	25.2673	5.3402	21.2052	4.1460	10.0687	7.8605	9.0894
4	20.4592	12.9455	6.2248	33.6928	4.8647	28.3155	4.1535	14.2016	7.2679	12.8298
5	24.5065	17.3575	5.9032	42.1670	4.4154	36.672	3.9802	18.4177	6.6780	16.7393
6	28.5869	21.7664	5.4973	50.6311	4.0109	44.1026	3.7361	22.6572	6.1267	20.7363
7	32.6769	26.1429	5.0817	59.0595	3.6554	52.2595	3.4761	26.8923	5.6288	24.7753
8	36.7659	30.4780	4.6895	67.4446	3.3459	60.4621	3.2253	31.1116	5.1866	28.8326
9	40.8494	34.7717	4.3325	75.7866	3.0772	68.6746	2.9937	35.3111	4.7966	32.8958
10	44.9259	39.0281	4.0129	84.0889	2.8434	76.8808	2.7841	39.4908	4.4530	36.9590
11	48.9951	43.2519	3.7289	92.3563	2.6392	85.0737	2.5961	43.6519	4.1499	41.0193
12	53.0576	47.4477	3.4767	00.5932	2.4601	93.2511	2.4281	47.7962	3.8817	45.0755
13	57.1138	51.6199	3.2527	108.8039	2.3020	101.4129	2.2779	51.9257	3.6433	49.1274
14	61.1644	55.7720	3.0531	116.9919	2.1619	109.5598	2.1433	56.0421	3.4306	53.1749
15	65.2102	59.9071	2.8746	125.1605	2.0369	117.6932	2.0224	60.1471	3.2400	57.2183
16	69.2515	64.0276	2.7144	133.3122	1.9250	125.8144	1.9135	64.2422	3.0684	61.2580
17	73.2891	68.1356	2.5701	141.4493	1.8242	133.9247	1.8150	68.3285	2.9132	65.2943
18	77.3233	72.2330	2.4395	149.5737	1.7330	142.0252	1.7256	72.4071	2.7723	69.3275
19	81.3546	76.3210	2.3209	157.6871	1.6502	150.1172	1.6441	76.4790	2.6440	73.3580
20	85.3832	80.4010	2.2129	165.7906	1.5748	158.2015	1.5697	80.5450	2.5267	77.3861
21	89.4095	84.4740	2.1141	173.8856	1.5057	166.2789	1.5015	84.6056	2.4190	81.4119
22	93.4338	88.5408	2.0234	181.9730	1.4423	174.3503	1.4388	88.6616	2.3199	85.4358
23	97.4562	92.6021	1.9400	190.0537	1.3839	182.4163	1.3809	92.7134	2.2284	89.4579
24	101.4770	96.6586	1.8629	198.1283	1.3299	190.4774	1.3274	96.7614	2.1436	93.4784
25	105.4963	100.7109	1.7916	206.1976	1.2800	198.5341	1.2778	100.8061	2.0650	97.4975
26	109.5142	104.7593	1.7255	214.2620	1.2335	206.5869	1.2317	104.8477	1.9918	101.5153
27	113.5310	108.8042	1.6639	222.3221	1.1903	214.6361	1.1887	108.8866	1.9235	105.5319
28	117.5466	112.8461	1.6065	230.3782	1.1499	222.6821	1.1485	112.9230	1.8597	109.5474
29	121.5613	116.8852	1.5528	238.4308	1.1121	230.7252	1.1109	116.9571	1.7999	113.5620
30	125.5751	120.9218	1.5026	246.4801	1.0768	238.7657	1.0757	120.9892	1.7438	117.5757

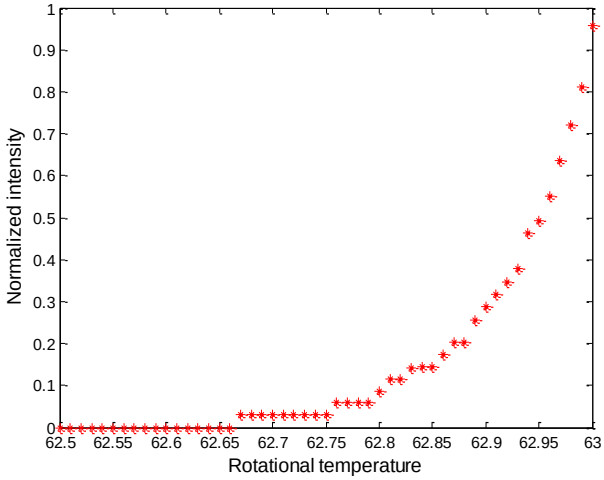

Figure 1: The average values of normalized intensities of the branches Q for Tr varying from 62.5 K to 63 K.

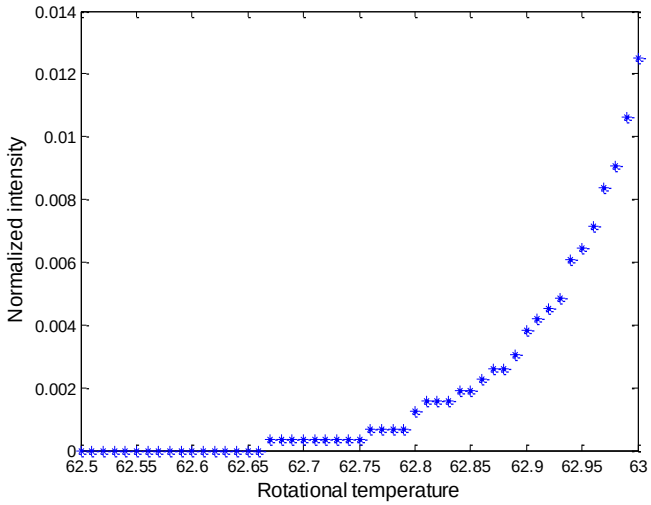

Figure 2: The average values of normalized intensities of the branches P for Tr varying from 62.5 K to 63 K.

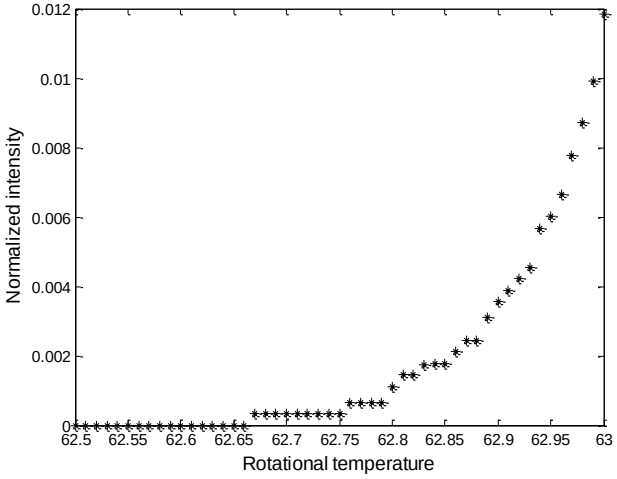

Figure 3: The average values of normalized intensities of the branches R for Tr varying from 62.5 K to 63 K.

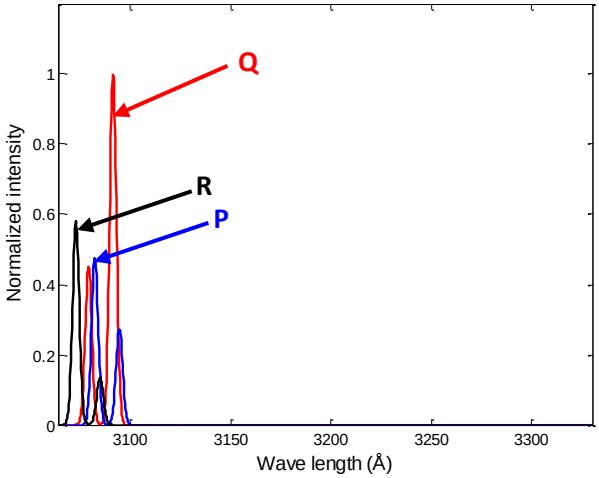

Figure 4: Emission spectra of Q, P and R branches for Tr=63 K.

To appreciate the level of sensitivity of the spectra of branches P, Q, and R to the rotational temperature, we represent the variation curves of the normalized average value of the intensity of branches Q, P and R as a function of the rotational temperature for Tr ranging between 100 K and 10,000,000 K (**Figures 5 to 10**). The results show that the emission spectra at Tr=100,000 K (**Figure 8**) is different to the one obtained at Tr=1,000,000 K (**Figure 9**). The superposition of these two curves shows it clearly in **Figure 11**. We can also note that the intensity of the branch Q has decreased despite the fact that temperature has been multiplied by 10. However, the obtained results at Tr=1,000,000 K (**Figures 9**) are identical to those obtained at Tr=10,000,000 K (**Figures 10**). The superposition of the two curves shows it clearly in **Figure 12**. The difference of the results at Tr = 100,000 K and Tr=1,000,000 K shows that there is a maximum limit temperature above which the spectra of the hydroxide radical is no longer sensitive to the variation of the rotational temperature.

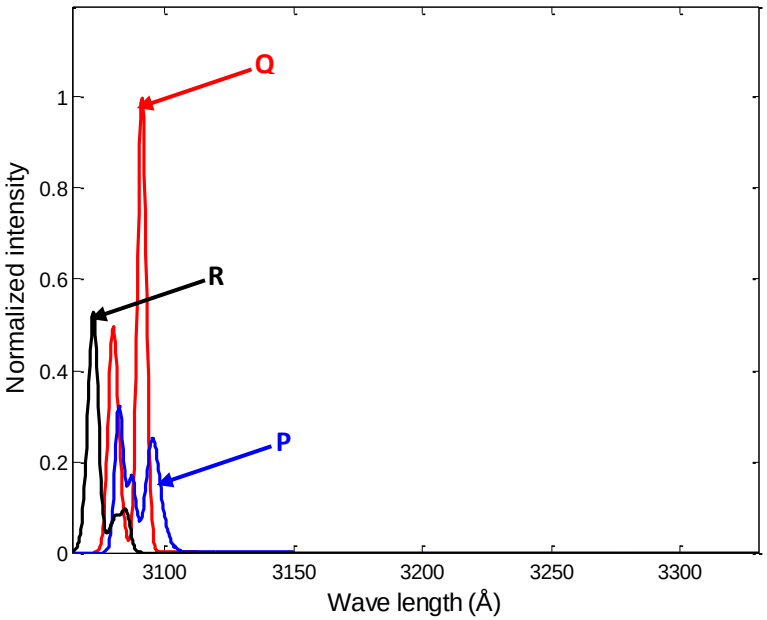

Figure 5: Emission spectra of Q, P and R branches for Tr=100 K.

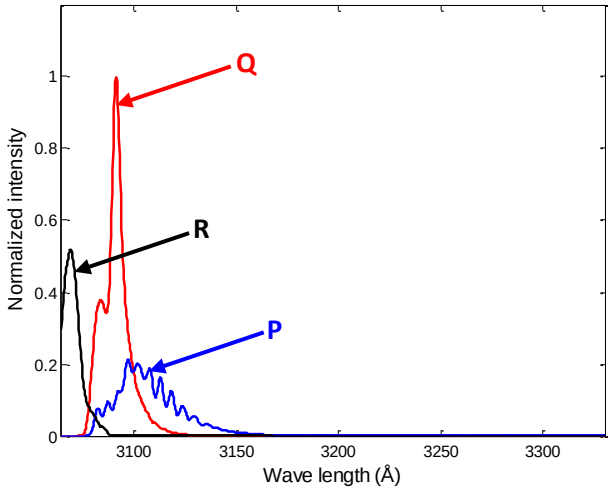

Figure 6: Emission spectra of Q, P and R branches for Tr=1000 K.

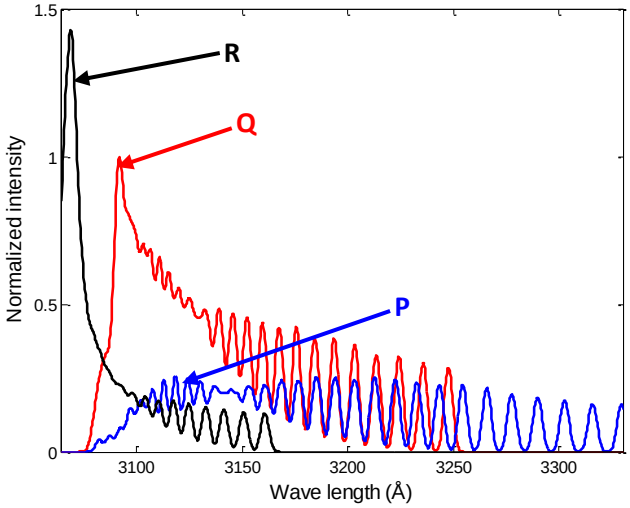

Figure 7: Emission spectra of Q, P and R branches for Tr=10,000 K.

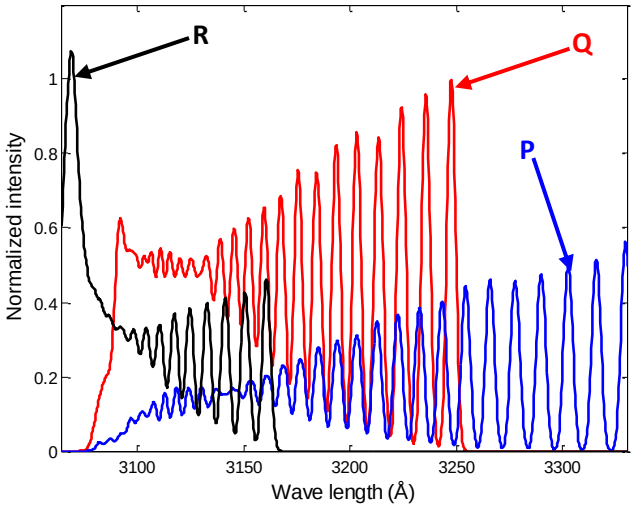

Figure 8: Emission spectra of Q, P and R branches for Tr=100,000 K.

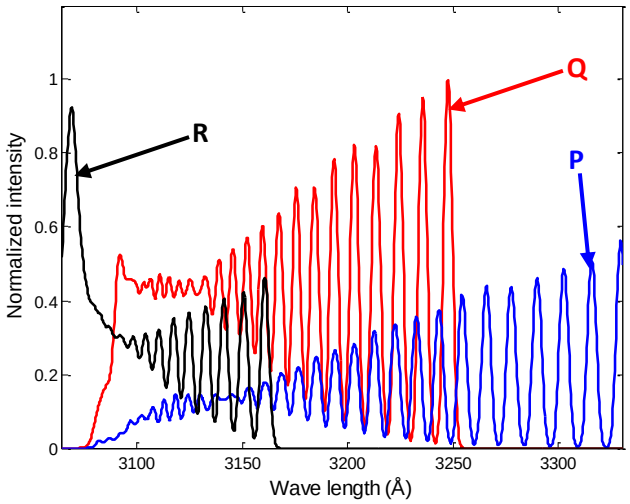

Figure 9: Emission spectra of Q, P and R branches for Tr=1,000,000 K.

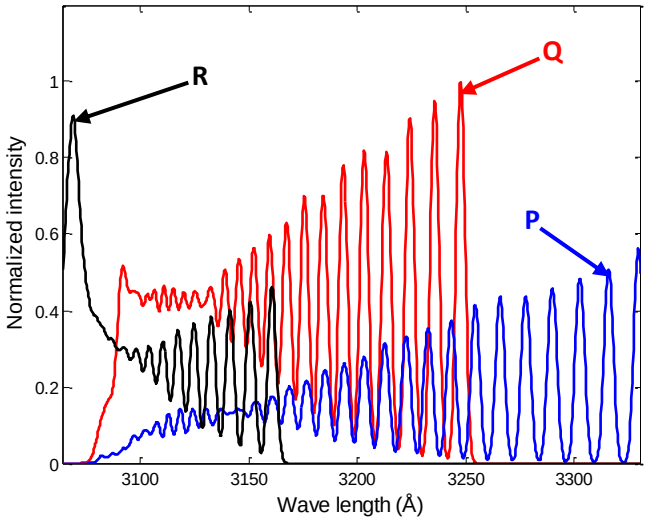

Figure 10: Emission spectra of Q, P and R branches for Tr=10,000,000 K.

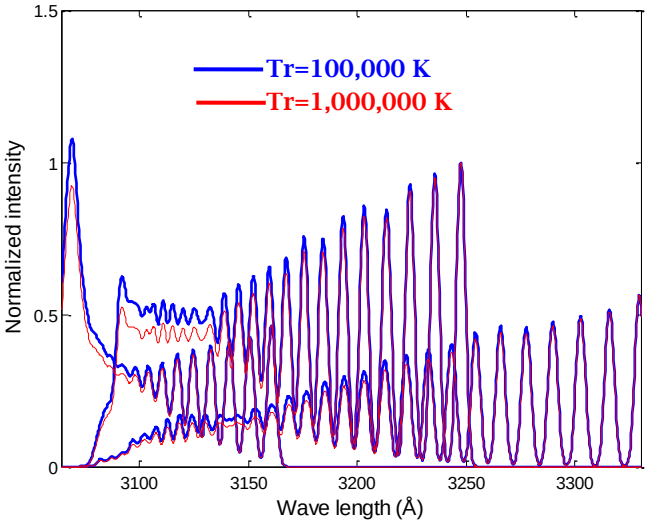

Figure 11: Overlay for Tr=100,000 K and Tr=1,000,000 K.

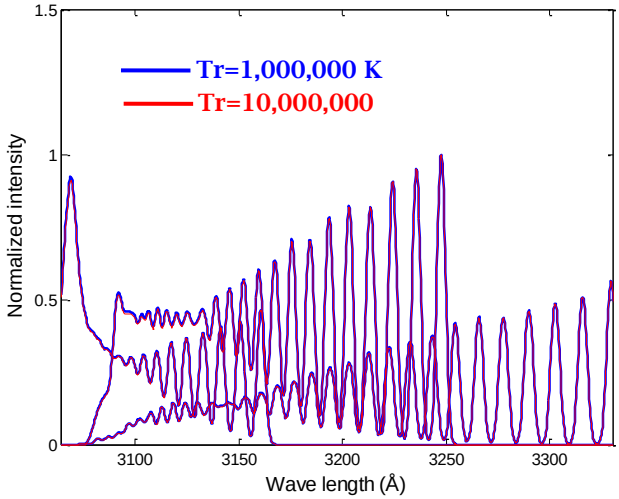

Figure 12: Overlay for Tr=1,000,000 K and Tr=10,000,000 K.

To determine the maximum value of temperature beyond which the branches P, Q, and R are no longer sensitive to the rotational temperature we present the normalized average values of the emission spectra of P, Q and R by varying Tr from 100,000 K to 1,000,000 K (**Figure 13**). We can notice that for all the three branches, the normalized average intensity increases from Tr=100,000 K to a maximum limit value noted T_r^{max}. Beyond T_r^{max} the normalized average intensity remains constant. The results of **Figure 13** show that the value of T_r^{max} is different for the 3 branches **(Table 4)**.

Finally, taking into account all the results presented in this article, we can highlight 3 major areas depending to the value of rotational temperature as shown in **Figure 14**. We can notice in this figure that:

- For $0 < T_r < T_r^{min}$: the emission spectra is not sensitive to the variation of Tr,
- For $T_r^{min} \leq T_r \leq T_r^{max}$: the emission spectra is sensitive to the variation of Tr,
- For $T_r > T_r^{max}$: the emission spectra is not sensitive to the variation of Tr.

The value of T_r^{max} is function to the nature of the branch as given in **Table 4**.

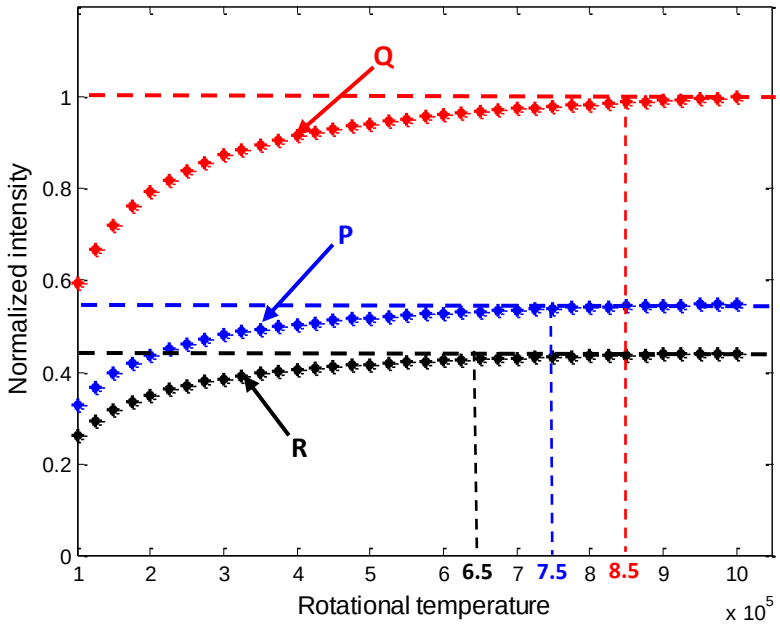

Figure 13: Average values of intensities of branches Q, P and R for 100,000 K ≤ Tr ≤ 1,000,000 K.

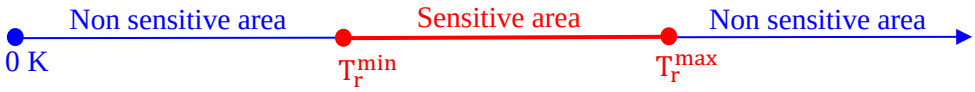

Figure 14: Areas of sensitivity of the spectrum of the P, Q and R branches to the rotation temperature.

Table 4: Sensitivity rotational temperature values.

Type of branch	Min temperature, T_r^{min} (K)	Max temperature, T_r^{max} (K)
Q	62.67	850,000
P	62.67	750,000
R	62.67	650,000

5. Conclusion

At the end of this study by normalizing all of the whole spectra relatively to the intensity of Q(0,0) and by varying the temperature of rotation from 0 K to 10,000,000 K we have shown that there is a range of rotational temperatures which influence the emission spectra of the branches Q, P and R of hydroxide radical OH. The lowest value of the rotational temperature is $T_r^{min} = 62.67$ K while the highest value noted T_r^{max} varies according to the nature of the branch. Indeed the results show that this maximum temperature is 850,000 K for the branch Q, 750,000 K for the branch P and 650,000 K for the branch R. We also note that when the rotational temperature varies from T_r^{min} to T_r^{max}, the heads of branches P, Q and R move before stabilizing for $T_r = T_r^{max}$. The normalized average intensity of each branch also varies before stabilizing near the sensitivity temperature.

6. References

[1] W Cowger, A Gray, S. H. Christiansen, H. De Frond, A. D. Deshpande, L. Hemabessiere, E. Lee, L. Mill, K. Munno, B. E. Ossmann, M. Pittroff, C. Rochman, G. Sarau, S. Tarby, and S. Primpke, "Critical Review of Processing and Classification Techniques for Images and Spectra in Microplastic Research," *Applied Spectroscopy*, Vol 74(9), 2020, pp. 989-1010.

[2] S. Ouoba, T. Daho, A. H. Yonli, and J. Koulidiati, "Spectroscopic study of the system of OH radical and determination of the rotational temperatures by using a numerical model," *J. Soc. Ouest-Afr. Chim.* Vol 38, 2014 pp. 22- 29.

[3] J. Koulidiati, A. Czernichowski, J. J. Beulens, and D. C. Schram, "Évaluation des températures de rotation et de vibration à partir du spectre d'émission A^2-$X^2\Pi$ de la molécule CH,". *Phys. Colloq. Phys*. (1990) C5 **51**, 297. *Colloque C5, supplément au n°18*, Tome 51, 1990, pp. 297-303.

[4] B. I. Takoua, B. Latifa, "Crystal Structure, Thermal Behavior and Vibrational Spectra of 4,4'Diamoniumdiphenylmethan Sulfate Hydrate," *Open Journal of Inorganic Chemistry*, Vol. 7, 2017, pp. 61-73.

[5] B. M. Krupp, "A new analysis of the $A^2\Delta$-$X^2\Pi$ system of CH" *The Astrophysical Journal*, Vol. 189, 1974, pp. 389-397.

[6] J. J. Beulens, C. Gastineau, N. Guerrassimov, J. Koulidiati, and D. C. Schram, "Atomic and molecular emission spectroscopy on an expanding argon/methane plasma," *Plasma Chemistry and Plasma Processing*, Vol. 14, 1994, pp. 15-42.

[7] N. Bolouki, J.-H. Hsieh, C. Li, and Y.-Z. Yang, "Emission Spectroscopic Characterization of a Helium Atmospheric Pressure Plasma Jet with Various Mixtures of Argon Gas in the Presence and the Absence of De-Ionized Water as a Target," *Plasma*, Vol. 2(3), 2019, pp. 283-293.

[8] C. Ni, and X. Cheng, "A*b initio* study of the second positive system of N_2 at high temperature," *Computational and Theoretical Chemistry*, Vol. 1197, 2021, 113158.

[9] M. Vardelle, S. Bansard, C. de Izarra, and H. Rabat, "Analysis of unresolved thermometric groups of rotational lines of the OH UV spectrum in the wavelength range 310-318 nm High Temperature Material Processes : *An International Quarterly of High-Technology Plasma Processes* (2005), DOI: 10.1615/HighTempMatProc.v9.i4

[10] J. Chapelle, S. Pellerin, J. M. Cormier, B. Pokrzywka, and K. Musiol, "Thermal condition control of an arc plasma CF4 reactor: swan band spectrum for temperature measurements," *High Temperature Material Processes: An International Quarterly of High-Technology Plasma Processes*, Vol. 1(2), 1997, pp. 273-285.

[11] A. Ehn, J. Zhu, X. Li, and J. Kiefer, "Advanced Laser-Based Techniques for Gas-Phase Diagnostics in Combustion and Aerospace Engineering," *Applied Spectroscopy*, Vol. 71(3), 2017, pp. 341-366.

[12] A. Gratien, E. Nilsson, J. F. Doussin, M. S. Johnson, C. J. Nielsen, Y. Stenstrøm, and B. Picquet-Varrault, "UV and IR Absorption Cross-sections of HCHO, HCDO, and DCDO," *J. Phys. Chem. A*, Vol. 111(45), 2007, pp. 11506–11513.

[13] L. Li, Y. Jiang, H. Ye, R. Q. Yang, T. D. Mishima, and M. B. Santos, "Low-threshold InAs-based interband cascade lasers operating at high temperatures," *Appl. Phys. Lett.*, Vol. 106, 2015, 251102.

[14] P. J. Cadusch, M. M. Hlaing, and S. A. Wade, "Improved Methods for Fluorescence Background Subtraction from Raman Spectra," *J. Raman Spectrosc*., Vol. 44(11), 2013, pp. 1587-1595.

[15] M. M. Smit-Miessen, "Intensity profiles of non-resolved CN bands," *Physica*, Vol. 9(2), 1942, pp. 193-212.

[16] T. Schädle, and B. Mizaikoff, "Mid-Infrared Waveguides: A Perspective," *Applied Spectroscopy*, Vol. 70(10), 2016, pp. 1625-1638.

[17] K. Kochan, D. E. Bedolla, D. Perez-Guaita, J. A. Adegoke, T. C. P. Veettil, M. Martin, S. Roy, S. Pebotuwa, P. Heraud, and B. R. Wood, "Infrared Spectroscopy of Blood," *Applied Spectroscopy*, Vol. 75(6), 2021, pp. 611-646.

[18] L. T. Earls, "Intensities in $^2\Pi$–$^2\Sigma$ Transitions in Diatomic Molecules," *Phys. Rev*., Vol. 48(5), 423 – Published 1 September 1935.

[19] G. H. Dieke, and H. M. Crosswhite, "The ultraviolet bands of OH: fundamental data," *J. Quant. Spectrosc. Radiat. Transfer. Pergamon Press Ltd. Printed in Great Britain*, Vol. 2, 1961, pp. 97-199.

[20] G. H. Dieke, H. M. Crosswhite, and B. Dunn, "Emission Spectra of the Doubly and Triply Ionized Rare Earths," *Journal of the Optical Society of America*, Vol. 51(8), 1961, pp. 820-827.

[21] R. C. M. Leaner, "The Influence of Vibration-Rotation Interaction on Intensities in the Electronic Spectra of Diatomic Molecules. I. The Hydroxyl Radical," *Proceedings of the Royal Society of London. Series A, Mathematical and Physical Sciences*, Vol. 269(1338), 1962, pp. 311-326.

[22] E. Hill, and J. H. Van Vleck, "On the Quantum Mechanics of the Rotational Distortion of Multiplets in Molecular Spectra," *Phys. Rev.*, Vol. 32, 250 – Published 1 August 1928.